

Received January 14, 2021, accepted February 20, 2021, date of publication February 26, 2021, date of current version March 8, 2021.

Digital Object Identifier 10.1109/ACCESS.2021.3062440

Designing a HVDC Insulation System to Endure Electrical and Thermal Stresses Under Operation. Part I: Partial Discharge Magnitude and Repetition Rate During Transients and in DC Steady State

HADI NADERIALLAF^{ID1}, PAOLO SERI^{ID1}, (Member, IEEE),
AND GIAN CARLO MONTANARI^{ID1,2}, (Fellow, IEEE)

¹Department of Electrical, Electronics and Information Engineering (DEI), University of Bologna, 40136 Bologna, Italy

²CAPS, Florida State University, Tallahassee, FL 32306-1058, USA

Corresponding author: Hadi Naderialla (hadi.naderialla@unibo.it)

ABSTRACT This paper has the purpose to investigate HVDC insulation design considering real operating conditions, when DC steady-state is affected by frequent voltage transients or load variations that may be present during all life. Electrical field distribution in insulation, and in insulation defects, may change significantly from DC steady-state when voltage and load vary with time, which can cause partial discharge activity often not been properly accounted for at the design stage. The Part I of this paper is dedicated to prove, through experiments, models and simulations, that electrical and thermal transients may incite partial discharges in defective insulations during cable energization, voltage polarity inversion at a constant nominal load, as well as during load variations at a constant nominal voltage. This can cause accelerated aging and premature breakdown even if the insulation system is designed properly to withstand DC electrothermal stress, without partial discharges in steady state, for all life, as it will be shown in Part II. Focus is on cables, but the approach described here is general for any DC insulation system.

INDEX TERMS Cable insulation, DC, voltage and load transients, design methodology, finite element analysis, partial discharges.

I. INTRODUCTION

DC insulation is not supposed to work all life under DC-steady state conditions, nor at constant thermal stress.

Voltage transients caused, e.g., by energization and voltage polarity inversions give rise to electric field transients that may last hours [1], [2]. Load variation, on the other hand, cause temperature transients inside insulation [3]. These transients, electrical and thermal, can be repeated many thousands of times during the insulation life.

The amount of damage that such transients can cause to insulation, and thus their contribution to premature failure, could be negligible if the rate at which they occur is small, or the insulation system design is conservative, and as

The associate editor coordinating the review of this manuscript and approving it for publication was Enamul Haque.

long as they are not triggering high aging-rate phenomena, as partial discharges. Inception of PD can degrade insulation locally, generating with time footpaths to insulation breakdown, so that failure can occur well in advance compared to the specified design life. This depends fundamentally on some factors which can be summarized by a damage concept: the longer PD are active and the higher the relevant energy (or power), the larger the contribution to life reduction [2]–[4].

During electrical and thermal transients, the electric field profile in insulation and internal defects may vary significantly. There might be a significant difference in field profile between the conductivity-driven distribution, in DC steady-state, [5], and the permittivity-driven one, which establishes at the beginning of voltage (and sometimes load) transients [2], [3]. PD might incite in insulation defects (cavities) during transients, but not in DC steady-state, if the insulation

is designed properly to work (at any operating temperature) at nominal voltages below the DC steady-state partial discharge inception voltage, $PDIV_{DC}$.

During transients, PD may have large repetition rate, as under AC sinusoidal voltage, and, therefore, constitute a source of non-negligible aging acceleration at the defect/insulation interfaces even if the transients last only minutes or hours. This can impact significantly on life when grid/asset component operation includes frequent voltage and load transients.

In [5] the authors considered insulation system design in DC steady-state, that is, when electric field transient rate is negligible during operation life.

Here, the conditions at which PD can occur during electrical and thermal transients are examined (Sections 2 and 3) and their repetition rate modelled. The feedback resulting from such potentially harmful phenomena on insulation system design is then presented and discussed in Part II of this work, with the aim of providing useful contributions to reliable DC insulation design.

II. ELECTRIC FIELD AND TEMPERATURE TRANSIENTS

A. ELECTRICAL CONDUCTIVITY MODELING

The steady-state dependence of electrical conductivity on temperature and electric field can be exploited using a well-known empirical model [3]–[6]:

$$\gamma_b(T(r,t), E(r,t)) = \gamma_0 e^{\alpha(T(r,t)-T_0)+\beta(E(r,t)-E_0)} \quad (1)$$

where γ_0 is the reference electrical conductivity at temperature T_0 (in °C) and reference electric field E_0 (in kV/mm). The temperature dependence of conductivity is delivered by coefficient α (in $^{\circ}\text{C}^{-1}$), whereas β (in mm/kV) accounts for the field dependence. It should be mentioned that the relationship with temperature has been approximated here by considering T in place of $1/T$, as it would be required referring to the Arrhenius equation [6]–[8]. In the usual operating temperature range of polymeric cables, and for typical values of α , this is an acceptable simplification (actually widely used).

B. DIELECTRIC TIME CONSTANT AND ELECTRIC FIELD TRANSIENT

The dielectric time constant for an insulating material is defined as the ratio of relative permittivity to electrical conductivity, as it can be derived from Maxwell equations, [3], [9], [10]:

$$\tau_d = \varepsilon_0 \varepsilon_{rb} / [\gamma_b(T(r,t), E(r,t))] \quad (2)$$

where ε_0 is the permittivity of free space ($8.85 \times 10^{-12} \text{ F.m}^{-1}$) and ε_{rb} is the relative permittivity of the dielectric material. The dielectric time constant for the medium filling the cavity can be obtained in the same way as (2) from general Maxwell equations, considering permittivities and conductivities of the cavity and of the dielectric connected in series [11].

In AC, the electric field intensification inside cavities embedded in the insulation will depend on the permittivity

of defect medium and dielectric. For a cylindrical cavity, the amplification factor is estimated by [12], [13]:

$$f_{AC} = E_c / E_b = \varepsilon_{rb} / \varepsilon_{rc} \quad (3)$$

where ε_{rc} and ε_{rb} are the relative permittivity, E_c and E_b are electric fields in the cavity and the insulating material, respectively.

Under steady-state DC conditions, the situation can be drastically different since the field inside a defect will depend on the conductivity ratio between the dielectric material and the medium filling the cavity. Therefore, the amplification factor for a cylindrical cavity is given by [3], [14]:

$$f_{DC} = E_c / E_b = \gamma_b(T(r), E(r)) / \gamma_c \quad (4)$$

where γ_c is the electrical conductivity of cavity medium (usually air, taken in the following as $3 \times 10^{-15} \text{ S/m}$, according to [14]).

Based on the dielectric time constant, τ_d , which can be calculated from (2), the field variation factor as a function of time, $f(t)$, from time 0 of a voltage or load transient to DC steady state condition, can be given by:

$$f(t) = f_{DC} + (f_0 - f_{DC}) \cdot \exp\left(-\frac{t}{\tau_d}\right) \quad (5)$$

where f_0 and f_{DC} are the values at the beginning and end of field or temperature transient, respectively.

For both electrical and thermal transients, f_{DC} is calculated from (4) under steady state condition. It must be noted that the value of f_{DC} in (5) varies with load and defect position in cable insulation, because of the thermal gradient which modifies conductivity along insulation radius (see (1)). In addition, f_{DC} can be higher or lower than f_0 depending on material properties and temperature (hence, load). The value of f_0 can be calculated in different ways for electrical or thermal transients.

For example, considering the energization of a cable, f_0 can be obtained from (3), since electric field is driven by permittivity just after voltage variation.

Regarding thermal transients and taking into account the properties of the typical insulating materials used at present for DC polymeric cables, the thermal time constant consequent to cable load variations is shorter than the dielectric time constant that drives e.g., cable energization with a DC voltage or voltage polarity inversion [3]. As a result, from the beginning of load variation to the end of thermal transient, electric field is always ruled by changes in conductivity. Thus, f_0 is also calculated from (4) as f_{DC} .

The electric field magnitude inside a cavity as a function of time, $E_c(t)$, can be then estimated, as a first approximation, by:

$$E_c(t) = E_{DC} + (E_0 - E_{DC}) \cdot \exp\left(-\frac{t}{\tau_d}\right) \quad (6)$$

In a cylindrical insulation geometry, the dielectric time constant in (6) can be estimated (from (2) and [11]) upon calculating/measuring the electrical conductivity under steady

state condition at the radius at which the cavity is located. For example, conductivity can be measured by flat specimens under equivalent temperature and electric field of the specified radius (which can be, in turn, estimated by analytical modelling or numerical simulation).

Equation (6) is a general model valid for both electrical and thermal transients upon defining E_0 , E_{DC} and selecting properly the transient time constant. For electrical transient, the capacitive electric field in a cavity immediately after a voltage change, E_0 , and the steady-state resistive condition, E_{DC} are given by:

$$E_0 = E_c(0^-) + \frac{U_0 \cdot \varepsilon_{rb}}{\varepsilon_{rb} \cdot h_c + \varepsilon_{rc} \cdot h_b} \quad (7)$$

$$E_{DC} = \frac{U_0 \cdot \gamma_b(T(r, t), E(r, t))}{\gamma_b(T(r, t), E(r, t)) \cdot h_c + \gamma_c \cdot h_b} \quad (8)$$

where $E_c(0^-)$ is the field immediately before the beginning of electrical transients which can be calculated from (8). U_0 is the amplitude of supply voltage at the end of voltage transient when it reaches to a constant value, h_b and h_c are thickness of insulation and cavity height, respectively.

C. THERMAL TIME CONSTANT AND THERMAL TRANSIENT

The thermal resistance and capacitance of a cylindrical insulation layer per unit length (thinking of an insulated cable) are given by [3], [15], [16]:

$$R_{th} = \ln\left(\frac{r_o}{r_i}\right) / 2\pi\lambda \quad (9)$$

$$C_{th} = \rho_m C_p \pi (r_o^2 - r_i^2) \quad (10)$$

where r_o and r_i are the outer and inner radius of insulation layer, respectively.

An accurate thermal time constant for DC cables can be calculated using Cauer-type ladder network, where each cable layer has its own thermal resistance and heat capacity [15], [16]. Due to the fact that the thermal conductivity of inner and outer conductor, as well as of the semiconducting layers, are significantly higher than that for cable insulation (and under the assumption of significant smaller thermal heat capacity of the conductor and semiconducting layer), their effect on the total thermal time constant of cable would be negligible. Therefore, the thermal time constant of a HVDC cable surrounded by air can be estimated with a good approximation by the thermal time constant of its electrical insulation layer [3]. When load is changed, the temperature across the cable insulation varies exponentially as a function of time [17], [18]:

$$\Delta T(t) = \Delta T_{ss} \left(1 - e^{-\frac{t}{R_{th}C_{th}}}\right) \quad (11)$$

where $\Delta T(t)$ is temperature variation with time, in K, ΔT_{ss} is the temperature gradient across the cable insulation layer at steady state in K, and $R_{th}C_{th}$ is thermal time constant, [3], [18], [19]:

$$\tau_{th} = R_{th}C_{th} \quad (12)$$

Considering the most common insulating materials used at present for DC polymeric cables (e.g., XLPE, PP), the thermal time constant characterizing cable load variations is shorter than the dielectric time constant of electrical transients, i.e., $\tau_{th} < \tau_d$. As explained in detail in [3], the consequence is that the electric field distribution inside both the cavity and the dielectric after a load variation will be ruled only by the consequent conductivity variation. Consequently, and as a first approximation, when $\tau_{th} < \tau_d$, both E_0 and E_{DC} in (6) can be calculated from (8), that is, under steady state condition. The supply voltage amplitude, U_0 , is considered constant during load variation from E_0 to E_{DC} , being load the unique cause of the field transient. Regarding the transient time constant in (6), when the load decreases, the transient time constant can be calculated from (2) where τ_d refers to the maximum load value (thus higher conductivity and shorter dielectric time constant). On the other hand, when the load increases, the thermal response is slower than that for cooling (see later Fig. 6). Thus, the transient time constant for heating is longer and it can be approximated roughly as $2\tau_d$ (which was verified also by COMSOL simulations), where τ_d is calculated from (2).

In some extreme conditions of low values of thermal conductivity, it can occur that the thermal constant reaches levels significantly higher than the dielectric time constant, i.e., $\tau_d \ll \tau_{th}$. In this case, the electric field might be driven not only by a change of conductivity with load, but also by permittivity, during the initial load variation transient. For this type of unusual conditions, the general model (6) applied to thermal transient can be valid for both heating (load rise) and cooling (load fall) conditions upon defining E_0 by an exponential model:

$$E_0 = E_m + (E_c(0^-) - E_m) \cdot \exp\left(-\frac{t}{2\tau_d}\right) \quad (13)$$

where $E_c(0^-)$ is the electric field just before the beginning of load variations calculated from (8). This converts (6) into a double exponential equation, that provides both an increasing phase of the field inside cavity just after load variation, and then a decreasing trend until steady state is reached [3].

E_m can be obtained by fitting models (6) and (13) to the simulated electric field by a numerical approach, and τ_d can be calculated from (2). This case, however, is not dealt with in the following.

D. PARTIAL DISCHARGE INCEPTION FIELD AND REPETITION RATE

To evaluate the partial discharge inception field, E_i , inside cavities embedded in insulations, we can refer to an approximate, deterministic expression proposed in [20] (for air in a spherical defect of diameter d):

$$E_i = 25.2p \left(1 + \frac{8.6}{\sqrt{pd}}\right) \quad (14)$$

where p is the gas pressure inside the cavity. This holds approximately also for cylindrical cavities, replacing d with cavity height, h_c , [2], [3], [5], [13], [21]–[23].

For voltage transients, the PD repetition rate as a function of time, $n(t)$, from beginning of the voltage transient (cable energization/voltage polarity inversion), n_0 , to DC steady state condition, n_{DC} , and can be estimated roughly as:

$$n(t) = n_{DC} + (n_0 - n_{DC}) \cdot \exp\left(-\frac{t}{\tau_{tr}}\right) \quad (15)$$

where n_{DC} corresponds to steady state condition and n_0 to the PD repetition rate in the initial instants of electric field variation, hence $n_0 = n(0^+)$. The transient time in (15), may not coincide with the dielectric constant, because of various factors involved in PD phenomenology and physics that can vary with time, such as inception and residual field (see (14) and (16)), memory effect due to space charge deposited by PD, modification of the medium and surface conditions in the discharging defect. Therefore, it is assumed $\tau_{tr} = C \cdot \tau_d$, being C an empirical constant value where $0.01 < C < 0.5$. Indeed, experimentally values of C mostly in the range 0.02 to 0.4 have been observed, depending on the electric field behavior during transient. If, for example, the transient field has non-monotone behavior, as it can be seen later in Fig. 2, PD can last a very short time.

PD repetition rate just after energizations or polarity inversions, n_0 , in (15) will be influenced by the slew rate of the applied voltage, and it can be roughly estimated by:

$$n_0 = \frac{1}{\Delta t} \cdot \left(\frac{|E_c(\Delta t)| - E_r}{E_i - E_r} \right) \quad (16)$$

where Δt is the time duration of the voltage variation from 0 to U_0 for energization or from U_0 to $-U_0$ (or vice versa) for polarity reversal, $E_c(\Delta t)$ is the maximum value of the electric field inside the cavity at the beginning of the transient (see e.g., next Fig. (2), E_i is the inception electric field from (14) and E_r is the residual electric field inside cavity after extinguishing each PD event.

The DC PD repetition rate, n_{DC} , in (15) under steady state DC condition can be defined and roughly approximated as [14]:

$$n_{DC} = \frac{\gamma_b(T(r,t), E(r,t)) \cdot h_c + \gamma_c \cdot h_b}{\varepsilon_{rb} \cdot (h_c + \varepsilon_{rc} \cdot h_b) \cdot \ln\left(\frac{|E_c(t)| - E_r}{|E_c(t)| - E_i}\right)} \quad (17)$$

It must be specified that (15) and (17) hold till $|E_c(t)| > E_i$, that is when PD can inception inside cavity considering a deterministic approach. Also, it must be pointed out that (15), (16) and (17) are again rough simplification of the reality, where a cavity may be not fully cylindrical, e.g., it can have non-negligible boundary effects, and PD can occur in different sections of the cavity surface (moreover, PD inception is stochastic rather than deterministic, as assumed in (14)).

Regarding the thermal transient, when $\tau_{th} < \tau_d$ the electric field is mostly ruled by conductivity. This influences PD repetition rate, which is closer to that characteristic to steady-state DC, that is, significantly lower, than the repetition rate during

TABLE 1. Geometry.

Parameter	Radius [mm]
Inner conductor	r_i
Inner semiconducting layer	r_{insemi}
Insulation layer	r_{insul}
outer semiconducting layer	$r_{outsemi}$
Outer conductor	r_{outcon}
Cavity height	h_c
Cavity cross section radius	r_c
	6

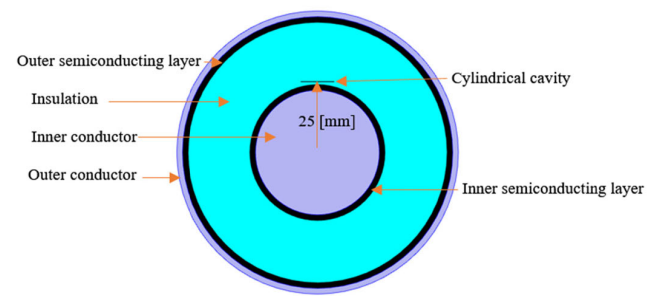


FIGURE 1. Cable geometry with cavity near the inner semicon.

voltage transients and AC, (16) [3]. Thus, in this case, DC PC repetition rate from beginning of load variation to the steady state condition can be calculated using (17).

The DC steady-state partial discharge inception voltage, $PDIV_{DC}$, can be estimated as [5], [22], [23]:

$$PDIV_{DC} = E_i \left(h_c + \frac{\gamma_c}{\gamma_b(T(r,t), E(r,t))} \cdot h_b \right) \quad (18)$$

where $\gamma_b(T(r,t), E(r,t))$ and E_i are obtained from (1) and (14), respectively. It should be mentioned that the value of $PDIV_{DC}$ obtained from (18) is the absolute value assumed to be constant for both positive and negative DC power supply.

Finally, AC partial discharge inception voltage, $PDIV_{AC}$, can be approximated as [5], [22], [23]:

$$PDIV_{AC} = E_i \left(h_c + \frac{\varepsilon_{rc}}{\varepsilon_{rb}} \cdot h_b \right) \quad (19)$$

It is noteworthy that in the above expressions of τ_d , the repetition rates, as well as of $PDIV_{DC}$, will depend on load and, therefore, the temperature gradient in the insulation. This is accounted in the models considering the location of the defect in the insulation, and the relevant temperature.

III. SIMULATION OF PD-OCCURRENCE LIKELIHOOD

A. MODELING AND SIMULATION

Coupled thermal and electric field simulations were implemented through the 2D axisymmetric model in COMSOL Multiphysics, referring to the two-dimensional cable geometry of Fig. 1 and insulating material parameters of Table 1. Using 2D axisymmetric model is the consequence of considering the cavity height for PD modelling, rather than cross

TABLE 2. Insulating material properties.

Parameter		Value
Heat capacity	C_p	1900 J/(kg.K)
Thermal conductivity	λ	0.38 W/(m.K)
Permittivity	ϵ_r	2.3
Reference electrical conductivity	γ_0	2E-17 [S/m]
Temperature dependency coefficient	α	0.1 [$^{\circ}\text{C}^{-1}$]
Field dependency coefficient	β	0.03 [mm/kV]

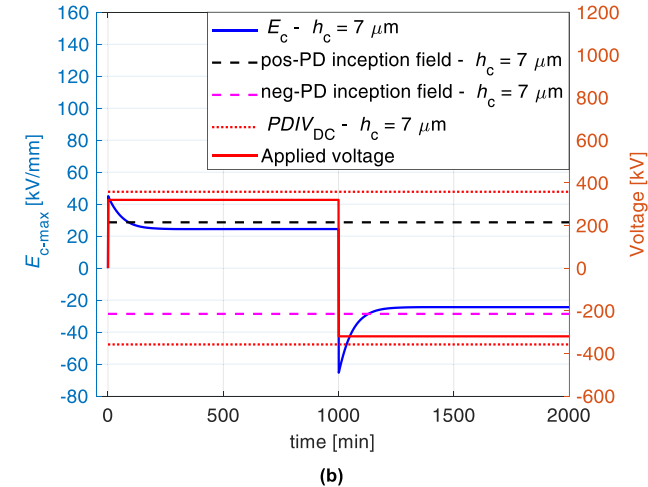
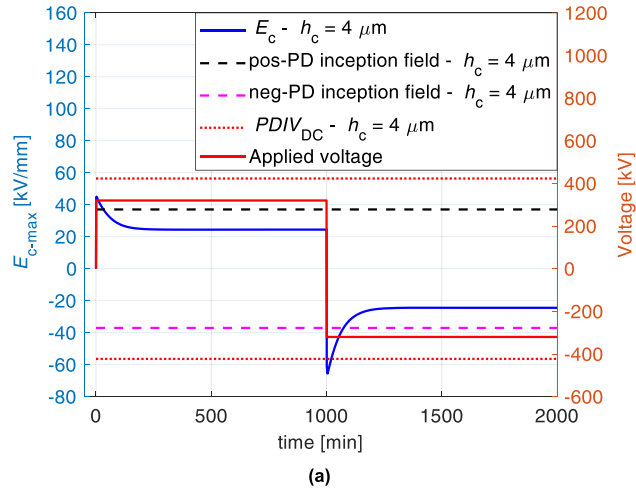


FIGURE 2. Simulated electric field variation inside a cavity during transient condition, after cable energization and voltage polarity reversal, to steady state DC condition as a function of time and cavity height, (a) $h_c = 4 \mu\text{m}$ and (b) $h_c = 7 \mu\text{m}$, ($T_0 = 0^{\circ}\text{C}$, $E_0 = 0 \text{ kV/mm}$ in (1)). PD inception field for two different cavity height values from (14), dashed lines, applied voltage and PDIV_{DC} from (18) are also indicated.

section and surface [3]. Referring to (14), since it is the height of a cylindrical cavity which plays the main role in determination of PD inception field [2], [3], [5], [13], [21]–[23], a rectangular geometry would be adequate to model the height of a cylindrical void in a 2D axisymmetric model.

To perform the simulations, a homogeneous cylindrical insulation layer is considered. The thermal and

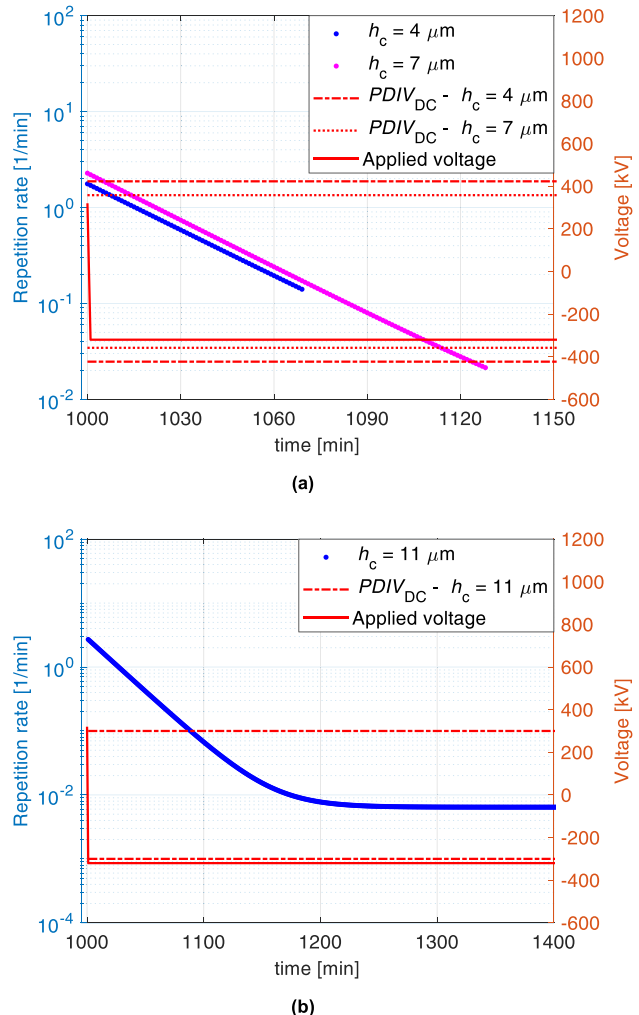


FIGURE 3. PD repetition rate as a function of time and cavity height following a polarity reversal, from (15), (16), and (17), where E_r is ignored. Applied voltage and PDIV_{DC} from (18) are also indicated. In Fig. 3a, curves stop at the time PD disappear, since the electric field in the cavity becomes lower than the inception field. (a) $h_c = 4$ and $7 \mu\text{m}$, and (b) $h_c = 11 \mu\text{m}$.

electrical properties of the implemented insulation material are parametrized in Table 2 [3], [8], [23].

Boundary conditions for thermal and electrical simulations, are parametrized in Table 3 [3], [24], assuming that the HVDC cable is surrounded by air and there is only convection heat transfer, while surface to ambient radiation (surface emissivity) in all directions is set to zero.

To mesh the model for both small and big cavity size, the sequence type and element size were set to physics-controlled mesh mode and extra fine, respectively.

In this study a cylindrical cavity near the inner semiconductor (precisely at 1 mm from the inner semicon), Fig. 1, is considered for the investigation. This is because, as proved in [3], the field inside a cavity near the inner conductor is always higher than that of a cavity of the same size near the outer semiconducting layer, and consequently, lower PDIV (thus, potentially more harmful). In addition, since the field is always driven by permittivity just after energizations, higher

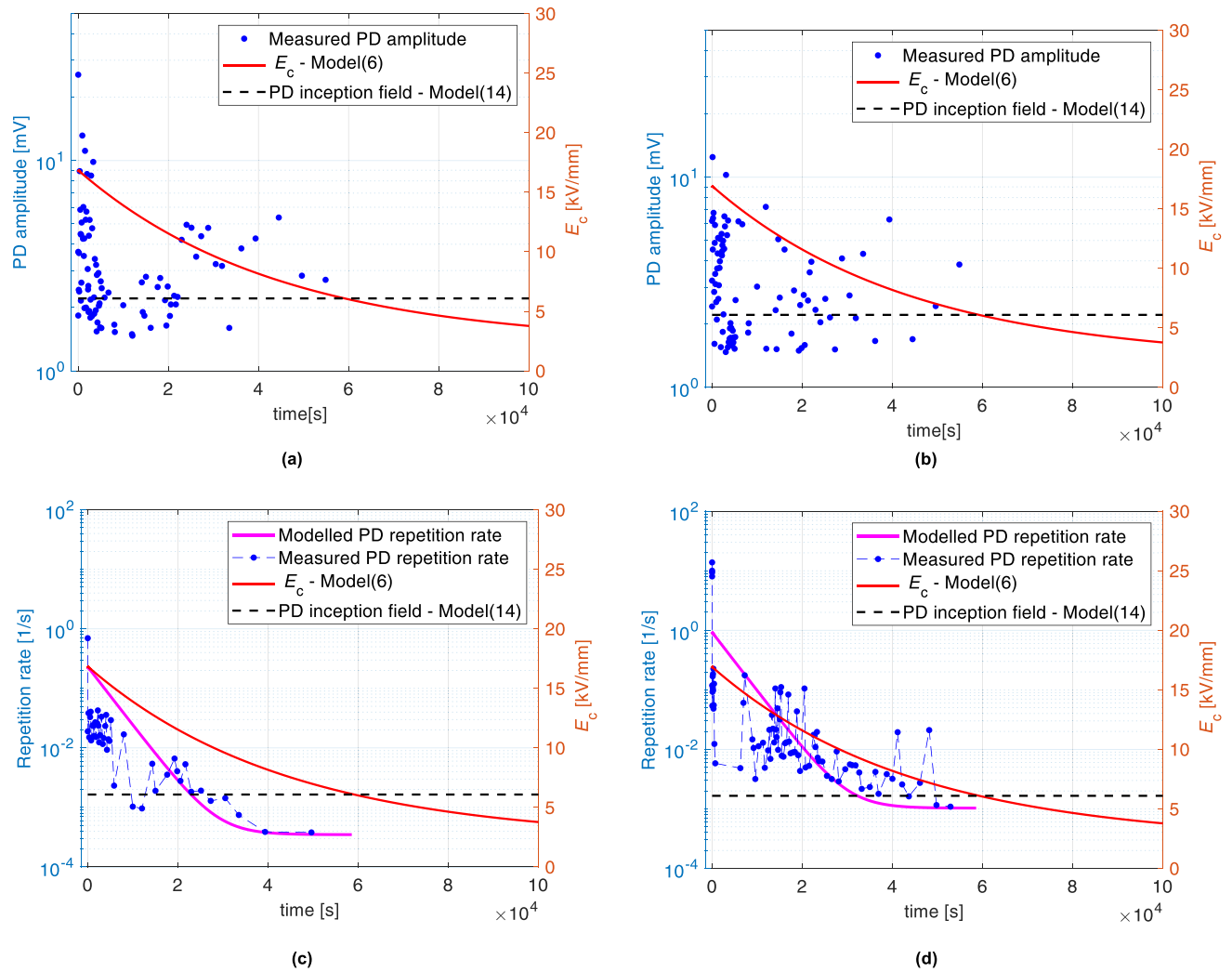


FIGURE 4. Experimental and modelling results (from (15), (16) and (17)) where E_r is neglected. PD testing upon energization for an insulation object with an internal cavity. PD amplitude with slew rate (a) 1 kV/s and (b) 4 kV/s, PD repetition rate as a function of time during energization transient with slew rate (c) 1 kV/s and (d) 4 kV/s. DC voltage, from 0 to 12 kV < $PDIV_{DC}$, room temperature, $\tau_d \approx 4.4 \cdot 10^4$ s and $\tau_{rr} \approx 0.1 \tau_d$. Electric field inside cavity from (6) and inception field inside cavity from (14) are also indicated.

TABLE 3. Boundary conditions and parameter values used for the reference HVDC cable simulation.

Parameter		Value
Nominal voltage	U_0	320 kV
Nominal load	I_0	1450 A
Voltage at outer conductor	φ_0	0 kV
Convection heat transfer coefficient	h	5 [W/(m ² .K)]
External temperature	T_{ext}	293.15 K

fields are expected in a cavity near the inner conductor also in those phases.

The effect of temperature dependence (α) and field-dependence coefficient (β) of electrical conductivity on PD activity are discussed in detail in [3], where it is shown that their high values (particularly α) lead to lower values of $PDIV$ and higher PD repetition rate.

B. PD DURING ELECTRIC FIELD TRANSIENT

In this section, the energization and voltage polarity reversal of a cable to 320 kV under full load is simulated, with a slew rate of 320 kV/min. The simulated electric field inside a cavity with two different heights (4 and 7 μ m) after energization and polarity reversal are illustrated in Fig. 2.

For both cavity heights, partial discharges can be inceptioned after energization and polarity reversals because the electric field in the cavity exceeds the PD inception field. Reaching the steady state field distribution, PD disappear after about 30 and 88 min from cable energization for $h_c = 4$ and 7 μ m, respectively, since the field becomes lower than the DC steady-state inception field. Indeed, in these cases $PDIV_{DC}$ is higher than the nominal voltage (see right vertical axes in Fig. 2). Longer duration of PD activity can also be noticed following a polarity reversal. Indeed, the simulation indicate that PD disappear after about 72 and 128 min from polarity

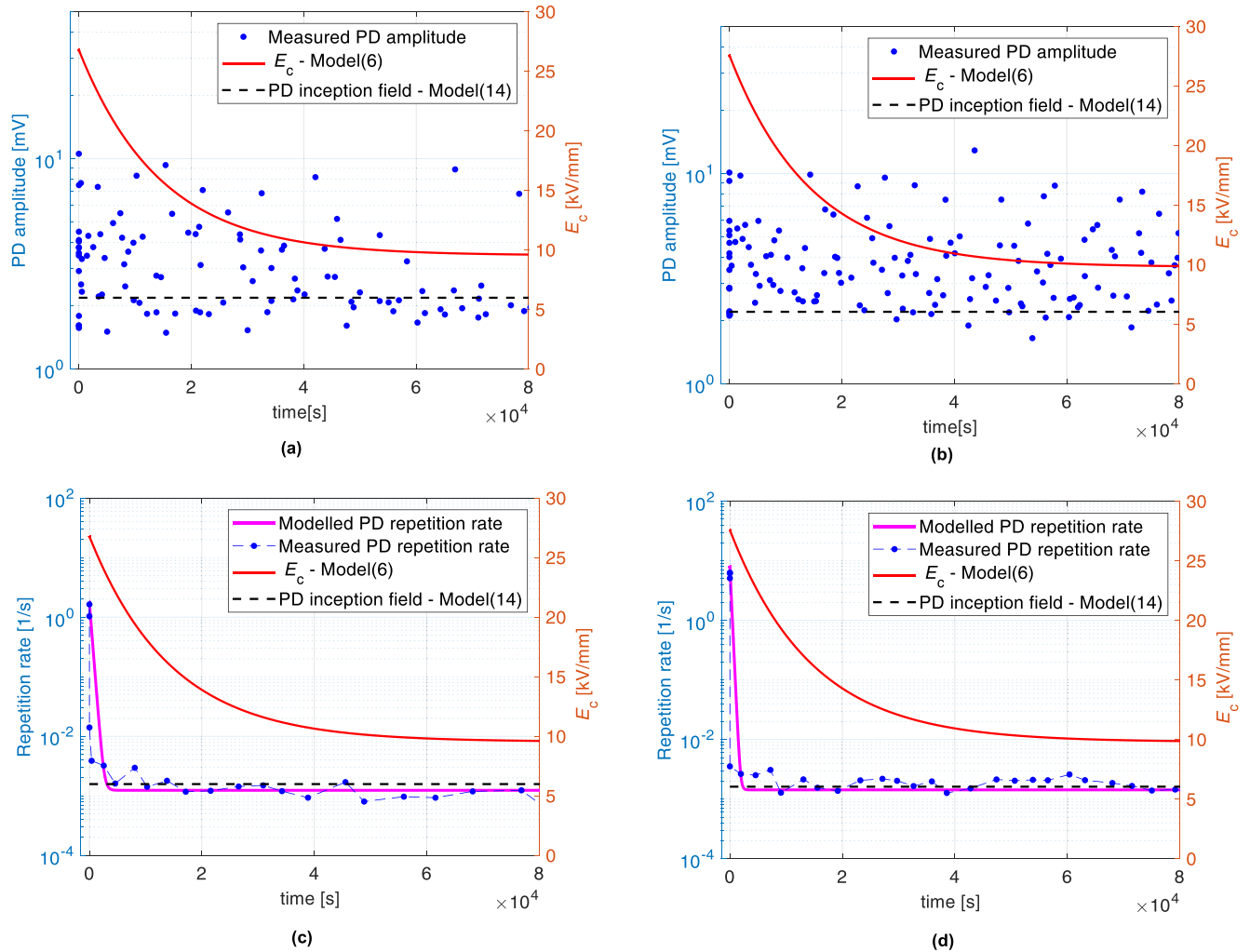


FIGURE 5. Experimental and modelling results (from (15), (16) and (17)) where $E_r = 0.9 E_i$ according to [13]. PD testing upon energization for an insulation object with an internal cavity. PD amplitude with slew rate (a) 1 kV/s and (b) 4 kV/s, PD repetition rate as a function of time during energization transient with slew rate (c) 1 kV/s and (d) 4 kV/s till steady state condition. DC voltage, from 0 to 20 kV $> PDIV_{DC}$, room temperature, $\tau_d \approx 1.4 \cdot 10^4$ s and $\tau_{rr} \approx 0.02\tau_d$. Electric field inside cavity from (6) and inception field inside cavity from (14) are also indicated.

inversion for $h_c = 4$ and 7 μ m, respectively. This is due to non-zero value of $E_c(0^-)$ characterizing polarity reversals (contrary to energizations), which leads to a higher electric field inside the cavity, according to (7) and longer duration of PD activity for this kind of events.

PD repetition rate values obtained by (15) for the cases of Fig. 2 after polarity reversal are displayed in Fig. 3a. Despite an almost equal electric field inside the cavity, a lower PD repetition rate is estimated inside cavities with smaller height for the considered cases. This can be explained by referring to the charging time constant of the equivalent circuit used to calculate PD repetition rate (see [14]), where smaller cavity height provides longer charging time constant, resulting in lower PD repetition rate.

In order to obtain DC PD also at steady state, the cavity height has to be increased to 11 μ m, providing a $PDIV_{DC}$ below the nominal voltage (see: Fig. 3b). In this case, DC PD repetition rate under steady state would be around

$6 \cdot 10^{-3}$ min $^{-1}$ from (17). It can be seen from Fig. 3b that after about 235 min (which is $3.5\tau_d$ and $9\tau_{rr}$, thus $\tau_{rr} \approx 0.4\tau_d$ as mentioned above) the repetition rate tends to that expected from DC. It should be mentioned that to simplify these simulations and result representation and discussion (reducing the number of parameters), E_r has been neglected. Considering higher values for E_r provides higher PD repetition rate values from (15), (16) and (17).

Values close to those calculated by simulations (i.e., having the same order of magnitude) were obtained experimentally. Two examples are shown in Figs. 4 and 5, which are taken from tests performed on multi-layer polypropylene specimens having a cylindrical cavity punctured on the middle layer (see [2]). Voltage was applied varying slew rate from 1 kV/s to 4 kV/s, up to values below or above $PDIV_{DC}$.

The results are shown for PD measurements during energization of a DC insulation system model (consisting of a multilayer specimen with internal cavities, typical of a

laminated cable). PD detection covered a bandwidth from 50 kHz to 100 MHz, fitting to the sensor used for the measurements, that is, a high-frequency current transformer (HFCT) sensor. The PD detector was endowed with an innovative, automatic, and unsupervised software which allows measurements and monitoring to be performed with any type of supply waveform, from power electronics to DC. The software has enhanced capability of noise rejection and PD identification also under DC supply voltage [25], [26]. The trigger level was 1 [mV] and a 1 [MHz] low pass filter was used to further reduce noise. PD measurement procedures for DC steady state and transient, including noise rejection and identification, were presented in [25].

Two different slew rate values are considered, with applied voltage $< PDIV_{DC}$ (Fig. 4) and $> PDIV_{DC}$ (Fig. 5). The cavity height values were 380 μm and 390 μm for Figs. 4 and 5, respectively. As can be seen, models for PD magnitude and repetition rate are not far from experimental results, considering, especially for amplitude, that PD is a stochastic phenomenon. PD inception indeed around the $PDIV_{AC}$ during the transient, when the electric field in the cavity reaches the inception value E_i from (14). Repetition rate (calculated by (15), (16) and (17)) fits to experiments quite well, both when PD do not occur in DC steady state (Fig. 4) and when the $PDIV_{DC}$ is lower than the applied voltage (thus PD are present in DC steady state): Fig. 5. Note that, according to the field behavior shown in Figs. 4c and 4d, the voltage rate of rise (slew rate) does not influence noticeably the electric field transient time, but it affects both initial PD charge amplitude (compare Figs. 4a and 4b) and PD repetition rate (Figs. 4c and 4d) just after electrical transient, when the field is driven by permittivity. Indeed, a higher slew rate (e.g., 4 kV/s) results in lower PD charge amplitude (Fig. 4b) as well as higher PD repetition rate (Fig. 4d) just after energization. In order to fit the repetition rate model to the experimental data under DC steady state condition, E_r was increased to $0.9E_i$ (Figs. 5c and 5d). As a result, E_r has a nonzero value under DC steady state condition, which cannot be ignored as already proved in [14].

Considering Figs. 4 and 5, it is verified that the modelled results are in good agreement with the experimental results within an order of magnitude.

C. PD DURING THERMAL TRANSIENT (LOAD CYCLING)

Simulations were carried out for a cable loaded with 10% of its nominal current (I_0) that is energized with nominal voltage (U_0). After reaching its thermal and electrical steady state ((2) and (12)), the cable is exposed to a periodic load cycling. The calculated electric fields for two different cavity heights are displayed in Fig. 6a. The load rises from 145 A to 1450 A at $t = 0$, then it is decreased again from 1450 A to 145 A at $t = 4000$ [min] (with the rate of 1450 A/min).

Reference was made to the more likely case of a thermal time constant (τ_{th}) shorter than the dielectric time constant (τ_d). As mentioned above, the thermal transient for conductivity variation is short enough that the field is driven by conductivity as in steady state DC. This case is highlighted

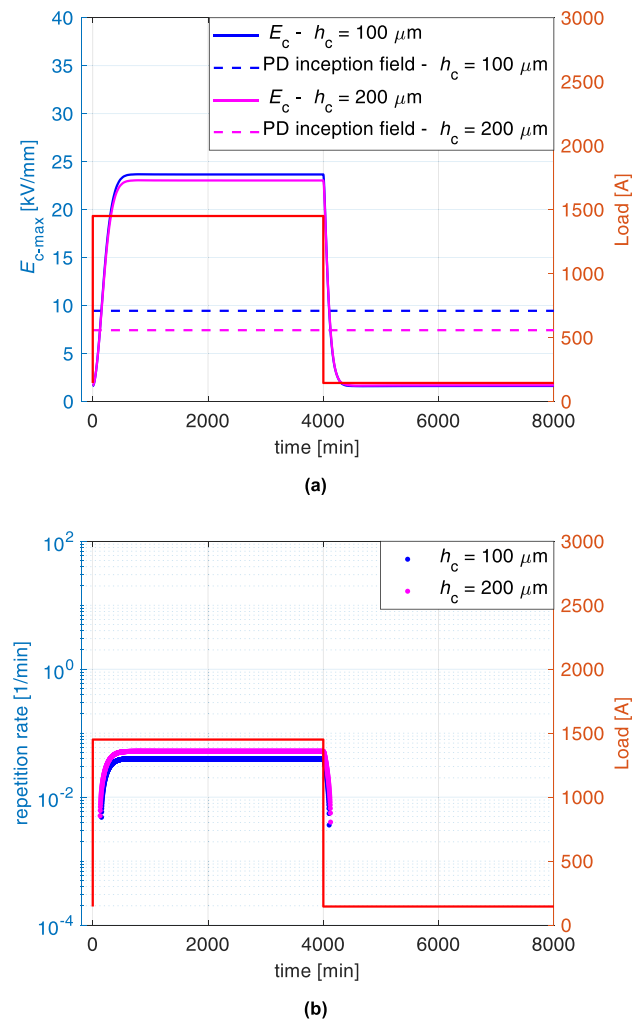


FIGURE 6. (a) Simulated electric field variation inside cavity from (6) when $\tau_{th} < \tau_d$ during one load cycle as a function of time and cavity height. PD inception field for two different cavity height values from (14) is indicated in Fig. 6a, and (b) PD repetition rate as a function of load cycle and cavity height during thermal transient and steady state condition from (17) where E_r is ignored. The load cycle is also indicated.

by Fig. 6, where electric field variation inside cavity and PD repetition rate during a load cycle from 10% to full load are reported considering an insulation with the parameter values of Tables I to III. As shown in Figs. 6a and b, PD are absent in steady state when the load is 10% because electric field inside the cavity is lower than the inception field, but they occur during transients as well as in steady state, when the cable is under full load, and the electric field exceeds the inception field. As can be seen in Fig. 6b, PD repetition rate is comparable with the DC PD repetition rate under steady state condition as illustrated already in Figs. 5c and 5d.

On the whole, it is clear that conditions can exist where PD can inception either during a thermal transient and in steady state, or only during a transient or, of course, not at all. This depends on the electrical and thermal properties of the dielectric, cavity size, the design field and temperature rating, thus on load.

IV. CONCLUSION

The cases of electrical and thermal transients, which have to be expected in a modern network, where operating conditions are dynamic, indicate without doubts that DC assets and grids need a type of design that is customized for a specific application. This means that designing an insulation system for modern DC electrical assets, especially those relevant to electrification transportation or renewable generation, requires the *a priori* knowledge of operating conditions of the specific application for which an insulation system is designed. Alternatively, performance classes depending on the voltage and load transient rate can be used, as it is already done with rotating machines fed by power electronics (see IEC 60034-18-41), where insulation systems can account for different levels of performance, such as heavy, medium, and low duty. The purpose of Part I of this paper is to open a discussion about how to generate proper specifications, having shown that both voltage and load transient can trigger extrinsic aging phenomena, that is, PD, which can be absent (due to proper design) in DC steady state and may contribute to increase aging rate.

Part II of this contribution will look at aging and life modeling, to provide a view of how much the transient conditions can affect aging rate and, thus, insulation system reliability.

REFERENCES

- [1] F. H. Kreuger, *Industrial High DC Voltage: 1. Fields 2. Breakdowns 3. Tests*. Washington, DC, USA: Delft University Press, 1995.
- [2] G. C. Montanari, P. Seri, S. F. Bononi, and M. Albertini, "Partial discharge behavior and accelerated aging upon repetitive DC cable energization and voltage supply polarity inversion," *IEEE Trans. Power Del.*, early access, Apr. 3, 2020, doi: [10.1109/TPWRD.2020.2984766](https://doi.org/10.1109/TPWRD.2020.2984766).
- [3] H. Naderiallaf, P. Seri, and G. C. Montanari, "Investigating conditions for an unexpected additional source of partial discharges in DC cables: Load power variations," *IEEE Trans. Power Del.*, early access, Oct. 21, 2020, doi: [10.1109/TPWRD.2020.3032800](https://doi.org/10.1109/TPWRD.2020.3032800).
- [4] G. C. Montanari, R. Hebner, P. Morshuis, and P. Seri, "An approach to insulation condition monitoring and life assessment in emerging electrical environments," *IEEE Trans. Power Del.*, vol. 34, no. 4, pp. 1357–1364, Aug. 2019.
- [5] G. C. Montanari, P. Seri, and H. Naderiallaf, "A contribution to everlasting electrical insulation for DC voltage: PD-phobic materials," *IEEE Access*, vol. 8, pp. 41882–41888, Feb. 2020.
- [6] L. A. Dissado and J. C. Fothergill, *Electrical Degradation and Breakdown in Polymers*. Chicago, IL, USA: Peregrinus Press, 1992.
- [7] M. Marzotto and G. Mazzanti, "The statistical enlargement law for HVDC cable lines Part 1: Theory and application to the enlargement in length," *IEEE Trans. Dielectr. Electr. Insul.*, vol. 22, no. 1, pp. 192–201, Feb. 2015.
- [8] R. Bodega, G. C. Montanari, and P. H. F. Morshuis, "Conduction current measurements on XLPE and EPR insulation," in *Proc. 17th Annu. Meeting IEEE Lasers Electro-Optics Soc.*, Oct. 2004, pp. 101–105.
- [9] G. Mazzanti and M. Marzotto, *Extruded Cables for High Voltage Direct Current Transmission: Advance in Research and Development* (Power Engineering Series). Hoboken, NJ, USA: Wiley, 2013.
- [10] P. Seri, R. Ghosh, H. Naderiallaf, and G. C. Montanari, "Investigating energization transients and the potentiality of partial discharge inception and damage in nanofilled polypropylene insulation for DC cables and capacitors," in *Proc. IEEE 4th Int. Conf. Condition Assessment Techn. Electr. Syst. (CATCON)*, Nov. 2019, pp. 1–5.
- [11] H. Naderiallaf, P. Seri, and G. C. Montanari, "On the calculation of the dielectric time constant of DC insulators containing cavities," in *Proc. IEEE CEIDP*, Vancouver, BC, Canada, Oct. 2021, pp. 1–5.
- [12] G. C. Crichton, P. W. Karlsson, and A. Pedersen, "Partial discharges in ellipsoidal and spheroidal voids," *IEEE Trans. Electr. Insul.*, vol. 24, no. 2, pp. 335–342, Apr. 1989.
- [13] A. Pedersen, G. C. Crichton, and I. W. McAllister, "The theory and measurement of partial discharge transients," *IEEE Trans. Electr. Insul.*, vol. 26, no. 3, pp. 487–497, Jun. 1991.
- [14] P. Seri, H. Naderiallaf, and G. C. Montanari, "Modelling of supply voltage frequency effect on partial discharge repetition rate and charge amplitude from AC to DC: Room temperature," *IEEE Trans. Dielectr. Electr. Insul.*, vol. 27, no. 3, pp. 764–772, Jun. 2020.
- [15] G. J. Anders, *Rating of Electric Power Cables in Unfavorable Thermal Environment*, New York, NY, USA: Wiley, 2005.
- [16] T. Worzyk, *Submarine Power Cables: Design, Installation, Repair, Environmental Aspects*. Berlin, Germany: Springer-Verlag, 2009.
- [17] B. M. Weedy, *Underground Transmission of Electric Power*. Hoboken, NJ, USA: Wiley, 1980.
- [18] I. Garniwa and A. Burhani, "Thermal incremental and time constant analysis on 20 kv XLPE cable with current vary," in *Proc. IEEE 8th Int. Conf. Properties Appl. Dielectr. Mater.*, Jun. 2006, pp. 566–569.
- [19] Y. Zhang, X. Zhou, H. Niu, X. Wang, Y. Tang, J. Zhao, and Yo. Fan, "Theoretical calculation and experimental research on thermal time constant of single-core cables," *High Voltage Eng.*, vol. 35, no. 11, pp. 2801–2806, Nov. 2009.
- [20] L. Niemeyer, "A generalized approach to partial discharge modeling," *IEEE Trans. Dielectr. Electr. Insul.*, vol. 2, no. 4, pp. 510–528, 1995.
- [21] P. Seri, G. C. Montanari, A. Albertini, S. F. Bonomi, and M. Albertini, "Comparing the results of increasing-voltage design and qualification life tests on HVDC and HVAC cables: The effect of voltage-step growth rate and insulation thickness factors," in *Proc. Conf. Electr. Insul. Dielectr. Phenomena (CEIDP)*, 2020, pp. 1–4.
- [22] G. C. Montanari, R. Hebner, P. Seri, and H. Naderiallaf, "Partial discharge inception voltage and magnitude in polymeric cables under AC and DC voltage supply," *Jicable*, vol. 2019, pp. 1–4, Jul. 2019.
- [23] H. Naderiallaf, A. Cavallini, F. Esterl, R. Plath, P. Seri, and G. C. Montanari, "Measuring partial discharges in MV cables under DC voltage: Procedures and results in steady state conditions," in *Proc. IEEE Electr. Insul. Conf. (EIC)*, Jun. 2020, pp. 1–4.
- [24] S. J. Frobin, C. Freye, C. F. Niedik, and F. Jenau, "Generic field simulation framework for HVDC cables," in *Proc. IEEE 2nd Int. Conf. Dielectr. (ICD)*, Jul. 2018, pp. 1–5.
- [25] P. Seri, H. Naderiallaf, R. Ghosh, and G. C. Montanari, "An approach to noise rejection and partial discharge separation in DC cable testing, during steady state and voltage polarity inversion transients," in *Proc. 8th Int. Conf. Condition Monitor. Diagnosis (CMD)*, Oct. 2020, pp. 1–8.
- [26] G. C. Montanari, R. Hebner, P. Seri, and R. Ghosh, "Self-assessment of health conditions of electrical assets and grid components: A contribution to smart grids," *IEEE Trans. Smart Grid*, early access, Oct. 2, 2020, doi: [10.1109/TSG.2020.3028501](https://doi.org/10.1109/TSG.2020.3028501).
- [27] L. Sanche, "Nanoscopic aspects of electronic aging in dielectrics," *IEEE Trans. Dielectr. Electr. Insul.*, vol. 4, no. 5, pp. 507–543, Oct. 1997.
- [28] L. Testa, S. Serra, and G. C. Montanari, "Advanced modeling of electron avalanche process in polymeric dielectric voids: Simulations and experimental validation," *J. Appl. Phys.*, vol. 108, Aug. 2010, Art. no. 034110.
- [29] G. C. Montanari, "A contribution to unravel the mysteries of electrical aging under DC electrical stress: Where we are and where we would need to go," in *Proc. ICD*, Jul. 2018, pp. 1–11.
- [30] S. Serra, G. C. Montanari, and G. Mazzanti, "Theory of inception mechanism and growth of defect-induced damage in polyethylene cable insulation," *J. Appl. Phys.*, vol. 98, Aug. 2005, Art. no. 034102.
- [31] L. Simoni, *Fundamentals of Endurance of Electrical Insulating Materials*, CLUEB, Bologna, Italy, 1983.
- [32] G. C. Montanari, "Notes on theoretical and practical aspects of polymeric insulation aging," *IEEE Electr. Insul. Mag.*, vol. 29, no. 4, pp. 30–40, Aug. 2013.
- [33] *Guide for the Statistical Analysis of Electrical Insulation Breakdown Data*, document I. 62539, 2007.
- [34] G. C. Montanari and D. Fabiani, "The effect of nonsinusoidal voltage on intrinsic aging of cable and capacitor insulating materials," *IEEE Trans. Dielectr. Electr. Insul.*, vol. 6, no. 6, pp. 798–802, Dec. 1999.
- [35] G. C. Montanari, D. Fabiani, and F. Ciani, "Partial discharge and aging of AC cable systems under repetitive voltage transient supply," in *Proc. IEEE Electr. Insul. Conf. (EIC)*, Jun. 2016, pp. 379–382.
- [36] P. Seri, L. Cirioni, H. Naderiallaf, G. C. Montanari, R. Hebner, A. Gattozzi, and X. Feng, "Partial discharge inception voltage in DC insulation systems: A comparison with AC voltage supply," in *Proc. IEEE Electr. Insul. Conf. (EIC)*, Jun. 2019, pp. 176–179.



HADI NADERIALLF was born in Mashhad, Iran, in April 1986. He received the M.Sc. degree in electrical engineering from the Leibniz Universität Hannover, Germany, in 2012. He is currently pursuing the Ph.D. degree with the University of Bologna, Italy, working on the EU project GRIDABLE. He did his master thesis at the Schering Institute of High Voltage Techniques and Engineering, Leibniz Universität Hannover. He has working experience for five years as a transformer fluid specialist. His main research interests include liquid and nanostructured solid electrical insulating materials, HVDC cables design, space charge measurement and analysis, ac and dc partial discharge detection and modeling, insulation systems for electrical machines, condition monitoring techniques, HV transformer asset management, DGA, and transformer oil reclamation.



PAOLO SERI (Member, IEEE) was born in Macerata, Italy, in June 1986. He received the M.Sc. degree in energy engineering and the Ph.D. degree in electrical engineering from the University of Bologna, in 2012 and 2016, respectively. Since 2017, he has been part of the Laboratory of Innovative Materials for Electrical Systems (LIMES), University of Bologna, as a Research Fellow, currently working on the topics of HVDC cables design, partial discharge detection and modeling, and characterization of dielectric materials. He is also an Assistant Professor with the Department of Electrical, Electronic and Information Engineering (DEI), Bologna University.



GIAN CARLO MONTANARI (Fellow, IEEE) has been a Full Professor of electrical technology with the Department of Electrical, Electronic and Information Engineering, University of Bologna, teaching courses on technology, reliability and asset management. He is currently a Research Faculty III with the Center for Advanced Power Systems (CAPS), Florida State University, USA, and Alma Mater Professor with Bologna University, Italy. Since 1979, he has been working in the field of aging and endurance of insulating materials and systems, diagnostics of electrical systems, asset management, and innovative electrical materials (magnetics, electrets, super-conductors, nano-materials). He has been engaged also in the fields of power quality and energy market, power electronics, reliability and statistics of electrical systems, and smart grid. He was the Founder and the President of the spin-off Techimp, established, in 1999. He is the author or coauthor of more than 800 scientific articles. He has been recognized with several awards, including the IEEE Ziu-Yeda, Thomas W. Dakin, Whitehead, Eric Forster, and IEC 1906 awards.

• • •